

Steady State Creep Behavior of Functionally Graded Composite by using Analytical Method

Ashish Singla
Department of Mech. Engg.
BGIET, Sangrur, Punjab

Manish Garg
Department of Physics
S.D. College, Barnala, Punjab

V.K.Gupta
Department of Mech. Engg.
Punjabi University Patiala,
Punjab

ABSTRACT

The Steady state creep behaviour of a functionally graded cylinder made of isotropic composite containing varying distribution of silicon carbide particles has been investigated by a mathematical model. The creep behaviour of the FGM is described by a Norton's Power law. The effect of varying distribution of SiC_p particles of creep stresses and creep rates in the FGM cylinder has been analyzed and compared with a cylinder, having uniform distribution of reinforcement. The study reveals that the increasing particle content in the cylinder, tangential and effective stresses increase near the inner radius but decrease near the outer radius. The strain rates in FGM cylinder decreases with the increase in SiC_p reinforcement. The magnitudes of tangential and radial strain rates in FGM discs are significantly lower than in a uniform composite disc.

Keywords

Functionally Graded Material, Cylinder, Creep.

1. INTRODUCTION

Functionally Graded Material (FGM) is a new class of materials in which the material properties are varying w. r. t. some positions coordinates. FGMs possess a number of advantages that make them superior as compare the traditional materials (Noda *et. al.*, 1998, Birma and Byrd, 2007). In most of these applications, cylinder is subjected to severe mechanical and thermal loads, causing significant creep and reducing its service life (Gupta and Pathak, 2001, Hagihara and Miyazaki, 2008 and, Tachibana and Iyoku, 2004).

Arya and Bhatnagar (1976) studied creep behaviour of thick-walled anisotropic cylinder subjected to internal and external pressures. The results obtained for the cylinder by considering anisotropic properties in cylinder were compared with those estimated for isotropic cylinder. Mishra and Samanta (1981) investigated creep response in an orthotropic thick-walled cylindrical shells operating at high pressure and temperature. It is observed that the temperature variation has a significant effect on the strain as well as the strain-rate, in the presence of anisotropy in the material. Shukla (1997) investigated stresses and strain in a cylinder subjected to internal pressure. It is observed that the presence of lesser value of compressibility at the internal surface reduces the stresses required for the initial yielding. Chen *et. al.* (2007) studied creep response of thick walled FG cylinder subjected to both internal and external pressures. It is observed that theoretical results are in good agreement with the analytical results obtained by using ABAQUS software. You *et. al.* (2007) analyzed effect of variation of material parameters on steady state creep in FGM cylinders subjected to internal pressure by using Norton's power law. Sharma *et. al.* (2010) estimated creep stresses in internally pressurized thick-walled rotating cylinder made of isotropic and transversely isotropic materials. It is observed that a transversely isotropic rotating

cylinder is on the safer side of the design as compared to a isotropic rotating circular cylinder made of isotropic material.

In the light of above mentioned, it has been decided to investigate the effect of varying reinforcement (SiC_p) gradient on the creep behavior of the FGM cylinder by using Norton Law. The study carried out is an attempt to evolve understanding of the creep behavior and content of the reinforcement on the creep stresses and strain rate in the FGM cylinder

2. DISTRIBUTION OF REINFORCEMENT

The distribution of SiC_p in the FGM cylinder decreases linearly from the inner to outer radius. The amount (vol %) of SiC_p, $V(r)$, at any radius r , is given by (Singh and Gupta, (2011).

$$V(r) = V_{\max} - \frac{(r-a)}{(b-a)} [V_{\max} - V_{\min}] \quad (1)$$

Where V_{\max} and V_{\min} are respectively the maximum and minimum content of SiC_p at the inner and the outer radii of the cylinder respectively

The average SiC_p content in the cylinder can be expressed as,

$$V_{\text{avg}} = \frac{\int_a^b 2\pi r l V(r) dr}{\pi(b^2 - a^2)l} = \frac{2 \int_a^b r V(r) dr}{(b^2 - a^2)} \quad (2)$$

Where l is the length of cylinder.

Substituting $V(r)$ from Eq. (1) into Eq. (2) and integrating, we get,

$$V_{\text{min}} = \frac{3V_{\text{avg}}(1-\lambda^2)(1-\lambda) - V_{\max}(1-3\lambda^2 + 2\lambda^3)}{2 - 3\lambda + \lambda^3} \quad (3)$$

Where $\lambda = a/b$

3. CREEP LAW AND PARAMETERS

The creep behavior of the FGM cylinder is described by Norton's power law as,

$$\dot{\epsilon}_e = B \sigma_e^n \quad (4)$$

Where $\dot{\epsilon}_e$ is the effective strain rate, σ_e is the effective stress, B and n are material parameters describing the creep performance in the cylinder.

It is evident from the study of Singh and Ray (2001) that the values of creep parameters B and n appearing in the Norton's law depend on the content of reinforcement, which vary with the radial distance.

$$B(r) = B_0 \left[\frac{V(r)}{V_{avg}} \right]^\phi \quad (5)$$

$$n(r) = n_0 \left[\frac{V(r)}{V_{avg}} \right]^{-\phi} \quad (6)$$

Where B_0 and n_0 are respectively the values of creep parameters B and n respectively and ϕ is the grading index. The values of B_0 , n and ϕ are respectively taken as 2.77×10^{-16} , 3.75 and 0.7 as reported in the study of Chen *et. al.*, (2007).

4. MATHEMATICAL FORMULATION

Consider a FGM thick-walled hollow cylinder with an inner radius a and outer radius b subjected to an internal and external pressures p and q respectively. The cylinder is made of orthotropic material and is sufficiently long and hence is assumed under plain strain condition (i.e. axial strain rate, $\dot{\epsilon}_z = 0$)

The radial ($\dot{\epsilon}_r$) and tangential ($\dot{\epsilon}_\theta$) strain rates in the cylinder are given by:

$$\dot{\epsilon}_r = \frac{d\dot{u}_r}{dr} \quad (7) \quad \text{and} \quad \dot{\epsilon}_\theta = \frac{\dot{u}_r}{r} \quad (8)$$

Where $\dot{u}_r = (du/dt)$ is the radial displacement rate and u is the radial displacement.

Eqs (7) and (8) may be solved to get the following compatibility equation,

$$r \frac{d\dot{\epsilon}_\theta}{dr} = \dot{\epsilon}_r - \dot{\epsilon}_\theta \quad (9)$$

The cylinder is subjected to the following boundary conditions,

$$\sigma_r = -p \text{ at } r = a \quad (10)$$

$$\sigma_r = -q \text{ at } r = b \quad (11)$$

Where the negative sign of σ_r implies the compressive nature of radial stress.

By considering the equilibrium of forces acting on an element of the cylinder in the radial direction, we get,

$$r \frac{d\sigma_r}{dr} = \sigma_\theta - \sigma_r \quad (12)$$

The material of the cylinder is incompressible, therefore,

$$\dot{\epsilon}_r + \dot{\epsilon}_\theta + \dot{\epsilon}_z = 0 \quad (13)$$

The constitutive equations under multi axial creep in an orthotropic cylinder, when the principal axes are the axes of reference, Bhatnagar and Gupta [2] are given by,

$$\dot{\epsilon}_r = \frac{\dot{\epsilon}_e}{2\sigma_e} [2\sigma_r - \sigma_\theta - \sigma_z] \quad (14)$$

$$\dot{\epsilon}_\theta = \frac{\dot{\epsilon}_e}{2\sigma_e} [2\sigma_\theta - \sigma_z - \sigma_r] \quad (15)$$

$$\dot{\epsilon}_z = \frac{\dot{\epsilon}_e}{2\sigma_e} [2\sigma_z - \sigma_\theta - \sigma_r] \quad (16)$$

Where $\dot{\epsilon}_e$ and σ_e are respectively the effective strain rate and effective stress in the FGM cylinder.

The Principal axes of isotropy are the axes of reference, Dieter [5], is given by,

$$\sigma_e = \left[\frac{1}{2} \left\{ (\sigma_\theta - \sigma_z)^2 + (\sigma_z - \sigma_r)^2 + (\sigma_r - \sigma_\theta)^2 \right\} \right]^{1/2} \quad (17)$$

Since Under plain strain condition ($\dot{\epsilon}_z = 0$), one may get from Eqs. (7), (8) and (13),

$$\dot{u}_r = \frac{C}{r} \quad (18)$$

Where C is a constant of integration. Using Eq. (18) in Eqs. (7) and (8), we get,

$$\dot{\epsilon}_r = -\frac{C}{r^2} \quad (19) \quad \text{and} \quad \dot{\epsilon}_\theta = \frac{C}{r^2} \quad (20)$$

Under plane strain condition, Eq. (16) becomes,

$$\sigma_z = \frac{(\sigma_r + \sigma_\theta)}{2} \quad (21)$$

Substituting σ_z from Eq. (21) in to Eq. (17), we get,

$$\sigma_e = \frac{\sqrt{3}(\sigma_\theta - \sigma_r)}{2} \quad (22)$$

Substituting $\dot{\epsilon}_r$ and σ_z respectively from Eqs. (19) and (21) into Eq. (14), we obtain,

$$\sigma_\theta - \sigma_r = \frac{1.33\sigma_e C}{\dot{\epsilon}_e r^2} \quad (23)$$

Using Eqs. (4) and (22) in Eq. (23) and simplifying, one gets,

$$\sigma_\theta - \sigma_r = \frac{I_1}{r^{2/n}} \quad (24)$$

Where, $I_1 = [1.33] \frac{n+1}{2n} \frac{C^{1/n}}{B^{1/n}}$ (25)

Substituting Eq. (24) into Eq. (12) and integrating, we get,

$$\sigma_r = X_1 - p \quad (26)$$

Where, $X_1 = \int_a^r \frac{I_1}{r^{n+2}} dr$ (27)

Substituting Eq. (26) into Eq. (24), we obtain,

$$\sigma_\theta = X_1 + \frac{I_1}{r^{2/n}} - p \quad (28)$$

To estimate the value of constant C , needed for estimating I_1 , the boundary conditions given in Eqs. (10) and (11) are used in Eq. (26) with X_1 (Eq. 27) integrated between limits a to b . to get,

$$\int_a^b \frac{I_1}{r^{n+2}} dr - p = -q \quad (29)$$

Substituting the value of I_1 from Eq. (25) in to Eq. (29) and simplifying, we obtain,

$$C = \left[\frac{p-q}{X_2} \right]^n \quad (30)$$

Where, $X_2 = \int_a^b \frac{(1.15)^{n+1}}{r^{n+2} B^n} dr$ (31)

Using Eqs. (21) and (22) into Eqs. (14) and (15), one obtains,

$$\dot{\epsilon}_\theta = -\dot{\epsilon}_r = \frac{\sqrt{3}\dot{\epsilon}_e}{2} \quad (32)$$

The analysis presented above yields the results for isotropic FGM cylinder.

5. NUMERICAL SCHEME OF COMPUTATION

Following the procedure described in section 4 and to begin the computation procedure, the values of X_2 Eq.(31) is estimated by substituting the value of the Creep parameters B and n from Eqs(5) and (6) respectively. To obtain the value of constant C by substituted the value of X_2 in Eq.(30) and using this value in Eq.(25), the value of I_1 is obtained. By using this value of I_1 in Eq.(27), the value of X_1 is obtained. After getting the value of X_1 , the Stresses σ_r and σ_θ are obtained from Eqs.(26) and (28) respectively. Now, to estimate the distribution of axial stress σ_z , the value of σ_r and σ_θ are substituted in Eqs.(21), after obtaining the value of σ_r, σ_θ and σ_z , the values of σ_e and $\dot{\epsilon}_e$ are calculated from Eqs. (22) and (4) respectively. Finally the strain rates $\dot{\epsilon}_r$ and $\dot{\epsilon}_\theta$ are calculated respectively from Eqs. (14) and (15). The results have been obtained for three different composite cylinders, as described in Table 5.1.

Table 5.1: Details of different composite cylinders

Cylinder	V_{max} vol. %	V_{avg} vol. %	V_{min} vol. %
Non-FGM (C1)	20	20	20
FGM (C2)	25	20	16
FGM (C3)	30	20	12

6. RESULTS AND DISCUSSION

Before presenting the result completed, it is necessary to check the validity of the analysis carried out. To accomplish this task, the tangential stress in a cylinder for which the results are reported by the Chen *et. al.*, 2007. The values of B_0 , n and ϕ are respectively taken as 2.77×10^{-16} , 3.75 and 0.7 as reported in the study of Chen *et. al.*, (2007). The tangential stress obtained in the cylinder is compared with that reported by Chen *et. al.* (2007). A good agreement (refer Fig. 1) is observed between the results obtained in present study and those of Chen *et. al.* (2007).

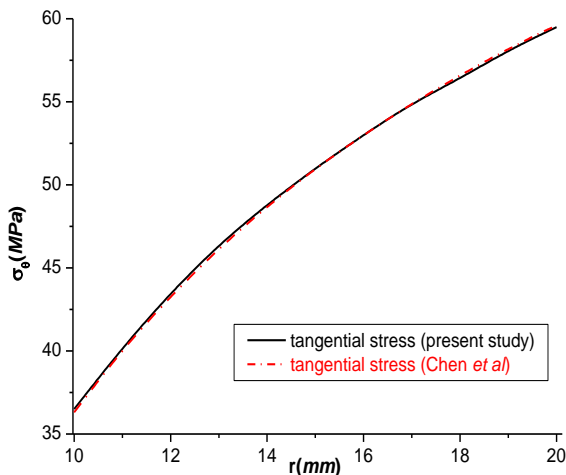


Figure.1: Validation of present study vs Chen *et. al.* (2007)

6.1 Variation of Creep Parameters

Figure 2 shows the variation of creep parameters B with radial distance in FGM and Non-FGM cylinders. In FGM cylinders C2 and C3, the value of parameter B decreases with increase in radius, but the value of B parameter remains constant for Non-FGM cylinder due to constant amount of SiC_p content. The variation of creep parameters B and n exhibits a crossover at a radius of around 15.8 mm. Figure 3 shows the variation of creep parameters n with radial distance in FGM and Non-FGM cylinders. In FGM cylinders C2 and C3, the value of parameter n increases with increase in radius, but the value of n parameter remains constant for Non-FGM cylinder due to constant amount of SiC_p content. Figure 4 shows the variation of SiC_p Content in FGM and Non-FGM cylinders. It is observed that the distribution of SiC_p reinforcement in FGM cylinder C2 and FGM Cylinder C3 decreases from inner to outer radius. However, the Non-FGM Cylinder C1 has uniform value because it remains 20% throughout. The variation of SiC_p Content exhibits a crossover at a radius of around 15.8 mm.

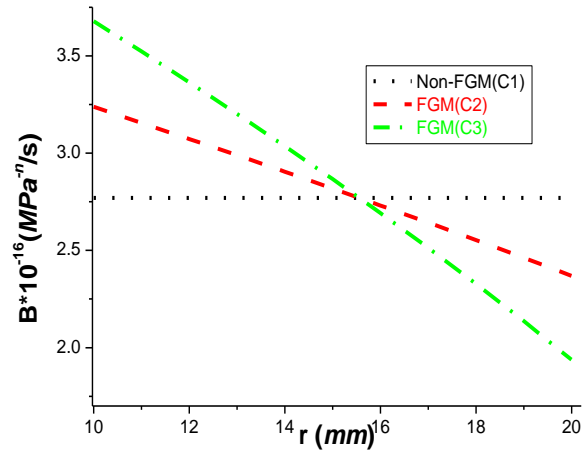


Figure 2: Variation of creep parameter B in cylinders

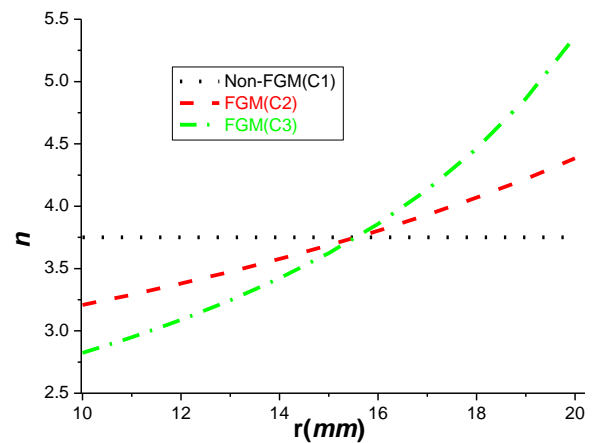


Fig.3: Variation of stress exponent n in cylinders

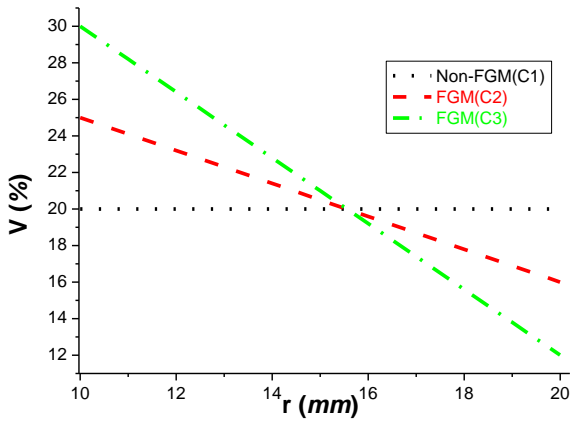


Fig.4: Variation of SiC_p Content in cylinders

6.2 Distribution of stresses and strains

Figure 5 shows the variation of radial stress in the FGM and Non-FGM cylinders. It is observed that the radial stress remain compressive over the entire cylinder with a maximum (compressive) and zero value reported at the inner and outer radii respectively, under the imposed boundary conditions given in Eqs. (10) and (11). It is observed which the radial stress is increasing over the entire cylinder radii with the increasing SiC_p reinforcement in the cylinder and the value of radial stress in FGM cylinder is higher than the Non-FGM Cylinder. Figure 6 shows the variation of tangential stress in the FGM and Non-FGM cylinders. The tangential stress remains tensile throughout the FGM and Non-FGM cylinders. By increasing Particle gradient in the FGM Cylinder, the tangential stress increases near the inner radius but decreases toward the outer radius when compared with the distribution of tangential stress in Non-FGM cylinder C1. At inner radius the value of stress of FGM cylinder C2 is less than FGM cylinder C3. Whereas at outer radius its vice versa i.e value of stress of FGM cylinder C2 is more than FGM cylinder C3. And the values of all these cylinders intersect each other in between 12.3 to 14.3. Figure 7 shows the variation of effective stress in the FGM and Non-FGM cylinders. It is observed that the effective stresses increase near the inner radius but decrease towards the outer radius, when compared with composite Non-FGM cylinder C1 having uniform distribution of SiC_p reinforcement.

Figure 8 shows the variation of radial and tangential strain rates in the FGM and Non-FGM cylinders. It is observed that the effect of radial and tangential strain rates in the cylinders decreases with increasing radius. The radial and tangential strains rates of Non-FGM cylinder C1 decreases as the radius increases, when Non-FGM cylinder C1 is compared with FGM cylinder C2 and C3, It is observed that in case of FGM Cylinder C2, the radial and tangential strain rates increases at inner radius and decreases at outer radius, while in case of FGM cylinder C3 the radial and tangential strain rate less than Non-FGM cylinder C1 and decreases as moves from inner radius to outer radius. Figure 9 shows the variation of effective strain rate in the FGM and Non-FGM cylinders similar those described for radial and tangential strain rates. The strain rates show a little decrease in the middle of the cylinder with the increase in SiC_p reinforcement.

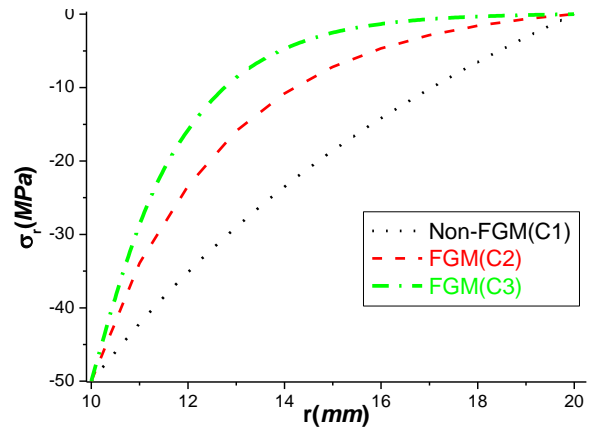


Fig.5: Variation of radial Stress in cylinders

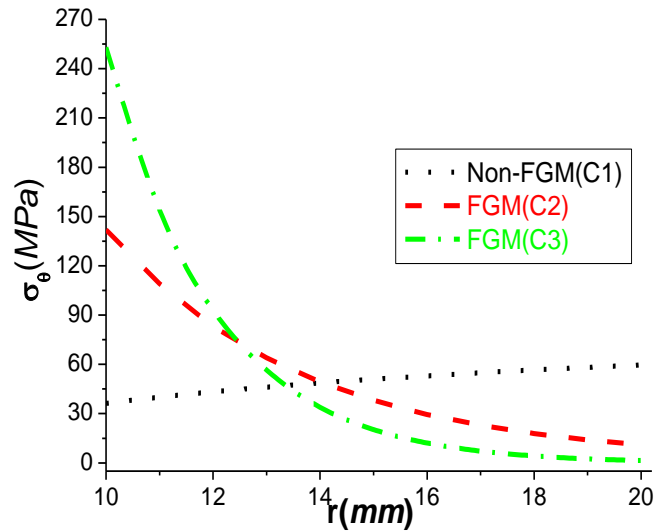


Fig. 6: Variation of Tangential Stress in cylinders

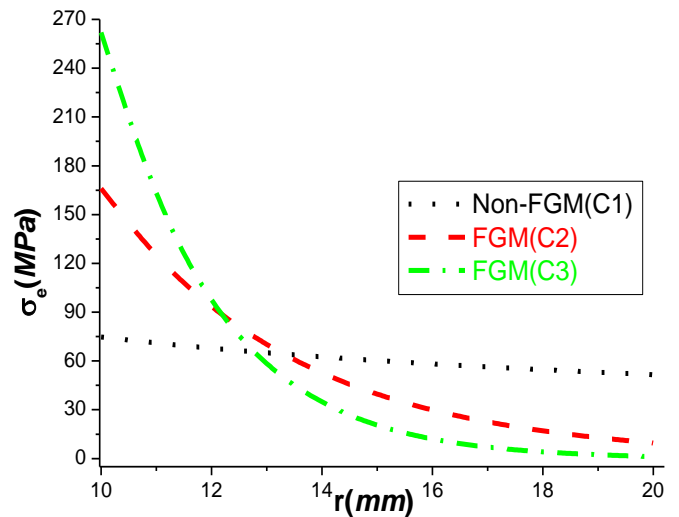


Fig. 7: variation of Effective Stress in cylinders

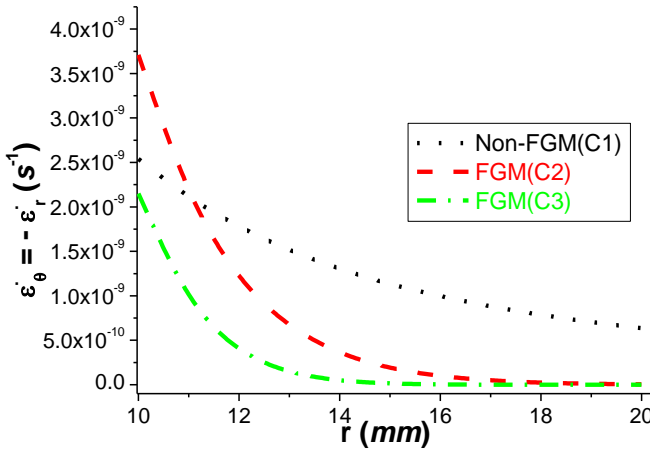


Fig. 8: variation of radial and tangential strain rate in cylinders

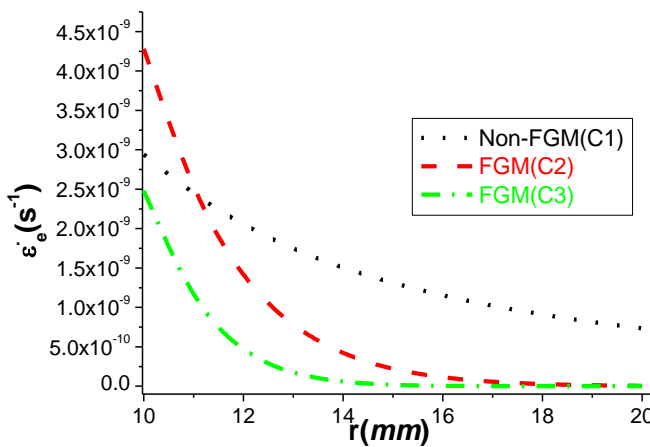


Fig. 9: Variation of effective strain rate in cylinders

7. CONCLUSIONS

The study carried out has led to the following conclusions:

- i. The radial stress (compressive) in the composite cylinder decreases throughout with the increase in particle gradient in the FGM cylinder. It is also observed that with the increase in SiC_p gradient in the FGM cylinder, the tangential and effective stresses increase near the inner radius but decrease towards the outer radius, when compared with cylinder having uniform distribution of SiC_p reinforcement.
- ii. The radial, tangential and effective strains in the composite cylinder decrease significantly with increasing SiC_p particle content in the cylinder. The reduction observed near the inner radius is more than those observed towards the outer radius. The strain rates show a little decrease in the middle of the cylinder with the increase in SiC_p reinforcement.

8. REFERENCES

- [1] Arya, V.K. and Bhatnagar, N.S. (1976) Creep of thick walled orthotropic cylinders subjected to combined internal and external pressures, Journal of Mechanical Engineering Science, Vol. 18, No. 1, pp. 1–5
- [2] Bhatnagar, N.S. and Gupta, S.K., (1969) Analysis of thick-walled orthotropic cylinder in the theory of creep, Journal of the Physical Society of Japan, Vol. 27, no. 6, pp. 1655- 1662
- [3] Birman, V. and Byrd, L. W. (2007) Modeling and Analysis of Functionally Graded Materials and Structures, Applied Mechanics Reviews, Vol. 60, pp. 195-216
- [4] Chen, J.J., Tu, S.T., Xuan, F.Z. and Wang, Z.D.(2007), Creep analysis for a functionally graded cylinder subjected to internal and external pressure, Journal of Strain Analysis of Engineering Design, Vol. 42, no. 2, pp. 69-77
- [5] Dieter, G.E. (1988) Mechanical Metallurgy, 3rd ed. London, McGraw-Hill Publications.
- [6] Gupta, S.K., Pathak, S. (2001) Thermo creep transition in a thick walled circular cylinder under internal pressure, Indian Journal of Pure and Applied Mathematics., vol. 32, issue. 2 , pp.237–253
- [7] Hagihara, S., and Miyazaki, N. (2008) Finite element analysis for creep failure of coolant pipe in light water reactor due to local heating under severe accident condition, Nuclear Engineering Design, Vol. 238, issue 1, pp. 33–40.
- [8] Mishra, J.C., and Samanta, S.C. (1981) Finite creep in thick walled cylindrical shells at elevated temperature, Acta Mechanica, Vol. 41, nos. 1-2, pp. 149-155
- [9] Noda, N., Nakai, S., Tsuji, T. (1998) Thermal stresses in functionally graded materials of particle-reinforced composite, JSME International Journal Series, Vol. 41, No.2, pp. 178-184
- [10] Shukla, R.K. (1997) Elastic-plastic transition in a compressible cylinder under internal pressure, Indian Journal of Pure and Applied Mathematics, Vol. 28, issue 2, pp. 277–288.
- [11] Singh, S.B. and Ray, S. (2001) Steady-state creep behavior in an isotropic functionally graded material rotating disc of Al-SiC composite, Metallurgical and Materials Transactions, Vol. 32, Issue. 7, pp. 1679-1685.
- [12] Singh, T. and Gupta, V.K. (2011) Effect of anisotropy on steady state creep in functionally graded cylinder, Composite Structures, Vol. 93, Issue 2, pp. 747-758.
- [13] Sharma S., Sahni M and Kumar R. (2010) Thermo creep transition of transversely isotropic thick-walled rotating cylinder under internal pressure, International Journal of Contemporary Mathematical Sciences, Vol. 5, no. 11, pp. 517 – 527
- [14] Tachibana, Y., Iyoku, T. (2004) Structural design of high temperature metallic components, Nuclear Engineering Design, vol. 233, Issue 1-3, pp. 261–272.
- [15] You, L.H., Ou, H. and Zheng, Z.Y. (2007) Creep deformations and stresses in thick-walled cylindrical vessels of functionally graded materials subjected to internal pressure, Composite Structures, Vol. 78, Issue 2, pp. 285–291.